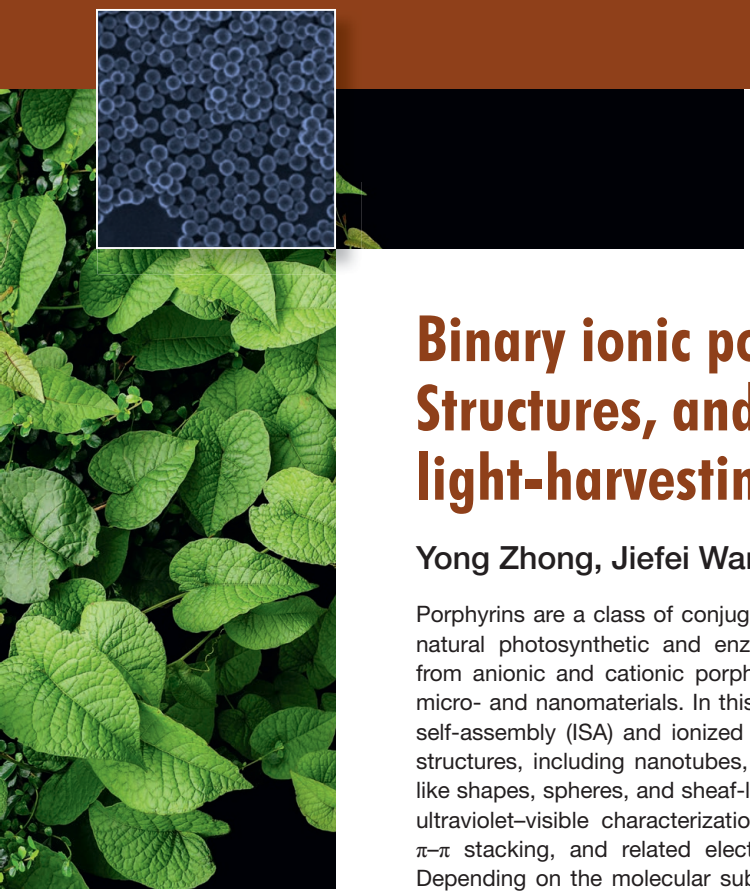


Binary ionic porphyrin self-assembly: Structures, and electronic and light-harvesting properties

Yong Zhong, Jiefei Wang, and Yongming Tian

Porphyrins are a class of conjugated molecules that structurally and functionally resemble natural photosynthetic and enzymatic chromophores. Crystalline solids self-assembled from anionic and cationic porphyrins yield a new class of multifunctional optoelectronic micro- and nanomaterials. In this article, we provide details on the concept of binary ionic self-assembly (ISA) and ionized forms of porphyrins, as well as formation of hierarchical structures, including nanotubes, rods and ribbons, sheets, and three-dimensional clover-like shapes, spheres, and sheaf-like structures. We summarize key physical properties from ultraviolet–visible characterizations of J-aggregate, exciton delocalization and extended π–π stacking, and related electronic and light-harvesting properties of the structures. Depending on the molecular subunits, the functionalities of the ISA materials are altered. These ISA nanostructures possess attractive light-harvesting and charge- and energy-transport functionalities and allow access to a novel class of nanomaterials with potential for applications in sensors, photovoltaics, photocatalysis, and solar power.

Introduction

Crystalline solids self-assembled from anionic and cationic porphyrins have received significant attention in nanoscience and nanotechnology.[1–3] Their tunable optical and electronic properties and their tailorable size and shape structures with molecular design provide an opportunity to control optoelectronic properties and device performance.[4] These structures show great promise for a variety of applications, including sensors,[5] energy-conversion and storage devices,[6] and light-harvesting energy materials for solar and other renewable energy systems.[7]

Porphyrins, which can be found in nature (e.g., chlorophyll), represent a class of conjugated organic molecules that possess unique planar, rigid molecular geometries, various metals (e.g., Cu, Zn, and Sn) that sit in the center of the ring for a metal porphyrin, and substituents (e.g., phenoxy and phenylcarboxy). These structurally and functionally resemble natural photosynthetic and enzymatic chromophores, which are parts of a molecule that are responsible for its color.[8] Porphyrins are attractive building blocks for self-assembled nanomaterials through noncovalent interactions, such as van der Waals forces, hydrogen bonding, aromatic π–π stacking, and axial coordination. Porphyrin assemblies are extensively being studied as promising organic photocatalytic, electronic, and biochemical phototherapy materials.

Self-assembled, porphyrin crystalline solids can be obtained by ionic, surfactant-assisted, phase-transfer self-assembly methods as well as other synthetic methods.[9–12] Here, we focus on the concept of binary ionic porphyrin self-assembly. This article summarizes the ionized forms of porphyrin, ultraviolet (UV)–visible optical absorption, and electronic and optoelectronic properties. Crystalline solid porphyrins self-assembled as photocatalytic organic semiconductors are also discussed, including the ability of photocatalytic reduction of metal complexes and deposition of metals onto their outer surfaces, photoreduction of H_2O to H_2, and the potential for light-driven CO_2-reduction catalysis with the aid of a soluble sacrificial electron donor (ED) under visible light.

Ionized forms of porphyrin

Binary ionic porphyrin self-assembly (ISA) is a method that uses binary, oppositely charged porphyrin ions to construct crystalline solids with defined size and morphology through electrostatic interactions and other noncovalent interactions,

Yong Zhong, Key Laboratory for Special Functional Materials, Ministry of Education, Henan University, China; zhywy8521115@163.com
Jiefei Wang, International Joint Center for Biomedical Innovation, Henan University, China; jfwang@henu.edu.com
Yongming Tian, Angstrom Thin Film Technologies LLC, USA; yongming.tian@gmail.com
doi:10.1557/mrs.2019.40

© 2019 Materials Research Society

https://doi.org/10.1557/mrs.2019.40 Published online by Cambridge University Press

such as van der Waals forces, hydrogen bonding, aromatic π–π stacking, and axial coordination in aqueous solution.[13,14] The morphologies and optoelectronic characteristics can be tuned by varying the substituent groups on the macrocyclic ring or using different center metals in the macrocycle cavity. ISA is becoming a significant synthetic route for constructing important porphyrin-based nanostructures and introducing properties that complement fluorescence imaging, photodynamic therapy, and magnetic resonance imaging.

Understanding ionized forms of porphyrin is crucial in order to regulate the structure. Metal-free porphyrins are excellent building blocks for the synthesis of multidimensional architectures. **Figure 1** summarizes the ionized states of tetraphenyl substituent groups (e.g., sulfonyl, carboxyl, pyridyl, methylpyridyl, amino) and metal-free porphyrins under different pH conditions in an aqueous environment, which are typically deduced from available pKa (the log of the acid dissociation constant) data.[15] pKa values of 4.8, 3.8, 2.2, 1.1, and 1 in aqueous solutions have been reported for tetra(4-sulfonatophenyl)porphyrin ($H_4(H_2TSPP)$ or TSPP), tetra(4-aminophenyl)porphyrin (H_2TAPP or TAPP), tetra (*N*-methyl-4-pyridyl)porphyrin ($H_2TMePyP$ or TMePyP, where Me is methyl), meso-tetra(4-pyridyl)porphyrin (H_2TPyP or TPyP), and tetra(4-carboxyphenyl)porphyrin ($H_4(H_2TCPP)$ or TCPP), respectively.

By deviating from the pKa value by controlling the acidity/basicity of the reaction medium, corresponding positively charged porphyrins and negatively charged porphyrins can be obtained. Then, one can manipulate the stoichiometry and morphology of the resulting ISA products. The introduction of central metals and metal ligands also affect the pKa value, thereby affecting the protonation state and the electronic structure of the porphyrin core. Elemental analysis has been performed on all starting materials and crystalline solids formed through porphyrin self-assembly, suggesting that the molar ratio of the binary porphyrins in the assembled structure corresponds to the charge of ionic stoichiometric ratios.[16]

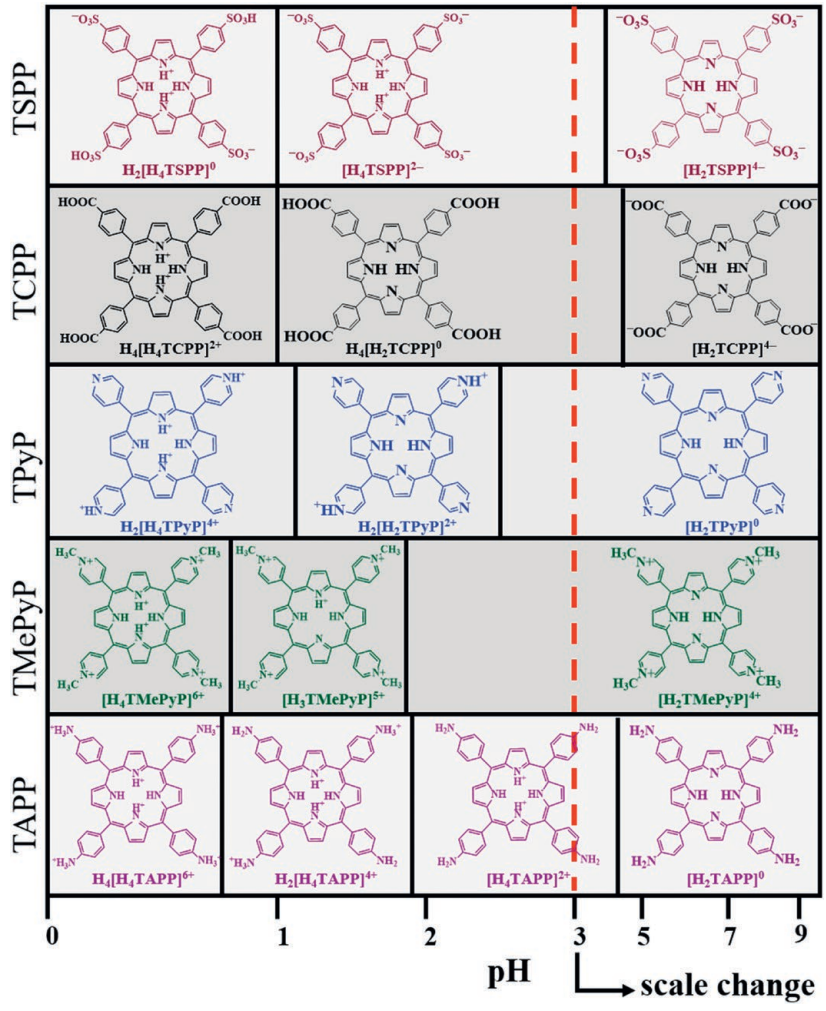


Figure 1. Protonation states of the TSPP, TCPP, TPyP, TMePyP, and TAPP porphyrin tectons (subunit building blocks) under different pH conditions based on pKa values. Ka is an acid dissociation constant and is a quantitative measure of the strength of an acid in solution. The more positive the value of pKa, where $pKa = -\log_{10}(Ka)$, the smaller the extent of dissociation at any given pH, that is, the weaker the acid. The scale change (red dashed line) indicates the reversal of the positive and negative charge with pH. Reprinted with permission from Reference 15. © 2016 World Scientific. Note: TSPP, tetra(4-sulfonatophenyl)porphyrin; TCPP, tetra(4-carboxyphenyl)porphyrin; TPyP, meso-tetra(4-pyridyl)porphyrin; TMePyP, tetra(*N*-methyl-4-pyridyl)porphyrin; TAPP, tetra(4-aminophenyl)porphyrin; Me, methyl; P, porphyrin.

Structure morphology from ionic porphyrin self-assembly

ISA is conducted through the coupling of two oppositely charged porphyrins (building blocks) by electrostatic interactions to prepare porphyrin nanostructures (see top schematic in **Figure 2**). Porphyrin nanotubes were formed by mixing equal volumes of a $H_4TPPS_4^{2-}$ solution (10.5 μM $H_4TPPS_4^{2-}$) and a Sn (IV) tetrakis (4-pyridyl) porphyrin dichloride (3.5 μM $SnTPyP^{2+}$) aqueous solution;[17] the mixture was left undisturbed in the dark at room temperature for 72 h. Hydrochloric acid (0.02 M HCl) is used to regulate the solubility and charge of porphyrin, and the individual porphyrins exhibit negligible aggregation at pH = 2. Then, the mixture of porphyrins immediately forms colloidal aggregates and provides a high yield (approximately 90%) of nanotubes (see Figure 2a). More interesting, the structure of tubes is highly controllable by modifying the center metal and the nature of the axial ligands.[17]

Since the first report of the ISA approach to synthesize porphyrin nanotubes, this method has been employed primarily for the preparation

https://doi.org/10.1557/mrs.2019.40 Published online by Cambridge University Press

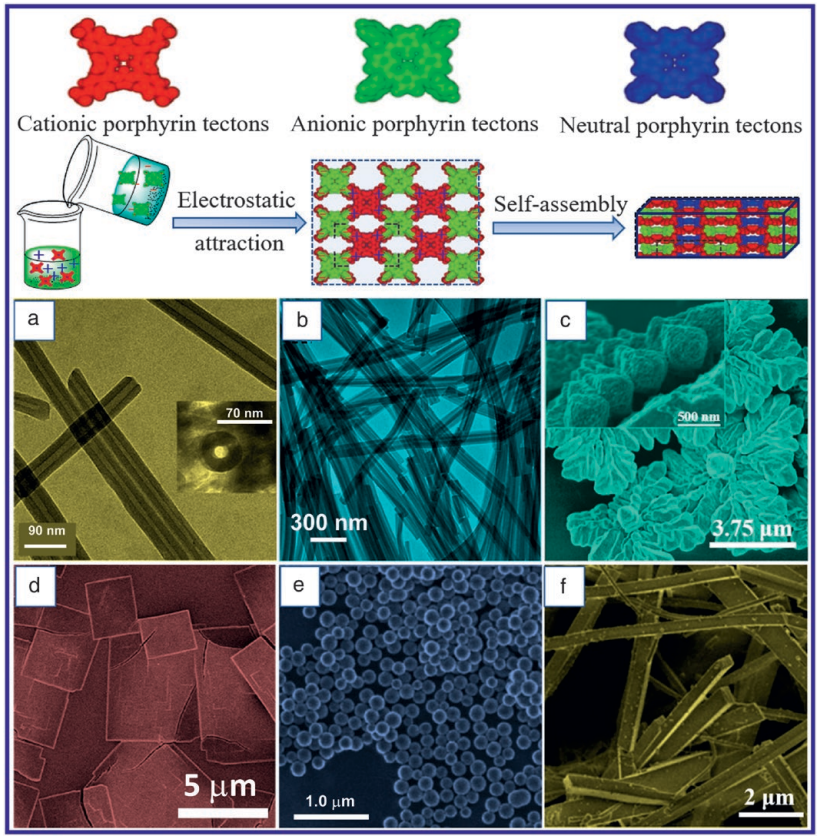


Figure 2. Top schematic: Ionic self-assembly (ISA) proceeds through coupling of two oppositely charged porphyrins (building blocks) by electrostatic interactions. ISA is a useful method for preparing porphyrin nanostructures.[25] (a) Transmission electron microscope (TEM) image of the porphyrin nanotubes. (Inset) Tube trapped in a vertical orientation by a thick mat of tubes. Reprinted with permission from Reference 17. © 2004 American Chemical Society. (b) TEM image of nanofiber bundles obtained by ISA of $(SbOTPP)^+$ and $(H_2TPPS_4)^{4-}$. Reprinted with permission from Reference 16. © 2006 Wiley. (c) Scanning electron microscope (SEM) image of the $SnTPPS^{4-}$ and $ZnT(N\text{-EtOH-4-Py})P^{4+}$ four-leaf clover-like structures. Inset: High magnification SEM image of a clover in an edge-on orientation. Reprinted with permission from Reference 18. © 2010 American Chemical Society. (d) SEM image of $CuTPPS^{4-}$ and $ZnT(N\text{-EtOH-4-Py})P^{4+}$ for a pH of 2.[21] (e) SEM image of SnT(4-Py)P:Pt coordination-polymer nanospheres that were undisturbed. Reprinted with permission from Reference 24. © 2009 Royal Society of Chemistry. (f) SEM image of SnT(4-Py)P:Pt coordination-polymer rods obtained when the reaction mixture was stirred. Reprinted with permission from Reference 19. © 2008 IOP Science. Note: SbOTPP, oxo-antimony (V) porphyrin; $(MTPPS_4)^{4-}$, water-soluble porphyrins (M = 2H, Sn, Cu, Ni, Ag, and Zn); $(H_2TPPS_4)^{4-}$, meso-tetrakis(4-sulfonatophenyl) porphyrin; $SnTPPS^{4-}$, Sn(IV) meso-tetrakis(4-sulfonatophenyl) porphyrin; $CuTPPS^{4-}$, Cu(II) meso-tetrakis (4-sulfonatophenyl) porphyrin; Et, ethyl; Py, pyridyl; P, porphyrin.

of various nanoscale porphyrin structures. ISA-induced phase-transfer reactions of the water-insoluble oxo-antimony (V) porphyrin $(SbOTPP)^+$ and the water-soluble porphyrins $(MTPPS_4)^{4-}$ (M = 2H, Sn, Cu, Ni, Ag, and Zn) were used to generate porphyrin nanofiber bundles (Figure 2b).[16] $(MTPPS_4)^{4-}$ aqueous solution was added to $(SbOTPP)^+$ dichloromethane solution and then vigorously stirred for 1 h. The liquid–liquid interface reestablished shortly, and pink material (rod-like nanostructures) immediately appeared in the organic phase. The rod-like nanostructures were uniform in size and shape at 70–140 nm wide and 1–2 μm long. According to energy dispersive spectroscopy microanalysis of the nanofiber bundles, the molar ratio of $(SbOTPP)^+$ to $(H_2TPPS_4)^{4-}$ was 3.7:1, close to the value of 4:1 that leads to neutralization of the charges of the ionic tectons, which are subunit building blocks. Additional studies have shown that a range of metalloporphyrins can be incorporated into nanofiber bundles when $(SbOTPP)^+$ mixes with the $(MTPPS_4)^{4-}$ of other center metals.[16]

Microscale four-leaf clover-shaped structures were formed by self-assembly of cationic tetra(*N*-ethanol-4-pyridyl)porphyrin ($ZnT(N\text{-EtOH-4-Py})P^{4+}$) and anionic tin (IV) tetrakis (4-sulfonatophenyl)porphyrin ($SnTPPS^{4-}$).[18] Scanning electron microscope images of the material (Figure 2c) revealed that the clovers are approximately square, with average edge lengths ranging from 2 to 10 μm and a few hundred nanometers thick. Interestingly, four leaves with well-defined "veins" (especially the midrib vein) were readily apparent as well as a central "stem" or "stalk" in high magnification (see inset in Figure 2c). All four combinations of these two metal complexes in the porphyrin macrocycle (Zn or Sn) resulted in similar clover-like structures, and the clover morphology varied with ionic strength and reaction temperature, but maintained fourfold symmetry. For example, when the pH = 2, the ISA of $CuTPPS^{4-}$ and $ZnT(N\text{-EtOH-4-Py})P^{4+}$ yielded nanosheets (Figure 2d).

Coordination chemistry, in combination with ion self-assembly of cation porphyrins and anion metal complexes, offers an array of novel functional nanostructure morphologies.[19] In this study, in the dark at room temperature, 5,10,15, and 20-tetrakis(4-pyridyl) metal porphyrin (SnT(4-Py)P, FeT(4-Py)P, or CoT (4-Py)P)HCl anion aqueous solution and the chloroplatinic acid (H_2PtCl_6) coordinating metal ions were rapidly mixed and then left undisturbed. Monodispersed solid nanospheres were formed in this undisturbed state, as shown in Figure 2e. When the reaction mixture was mixed under stirring, the product was changed to rods as shown in Figure 2f.

Optical and electronic properties of ISA porphyrin nanostructures

Porphyrin J-aggregates, a type of dye, possess electronically coupled and delocalized excitons in stacks. UV–visible absorption spectroscopy provides insights into the interactions and properties of ISA nanostructures. **Figure 3**a shows the UV–visible absorption spectra of the $H_4TPPS^{2-}/SnTHPyP^{4+/5+}$ nanotubes and the corresponding monomeric porphyrins.

https://doi.org/10.1557/mrs.2019.40 Published online by Cambridge University Press

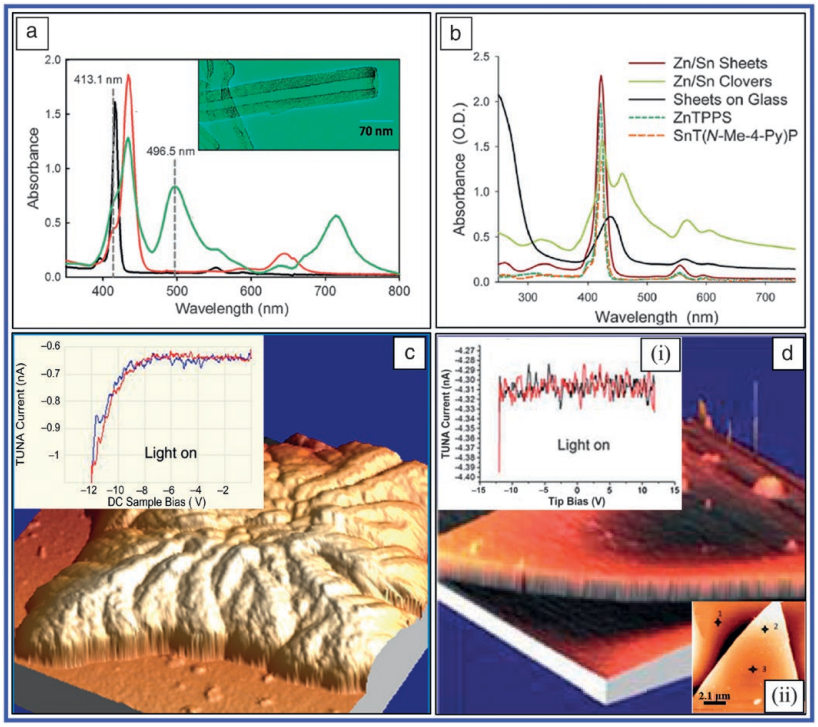


Figure 3. (a) UV–visible absorption spectrum of H_4TPPS^{2-}/SnTHPyP$^{4+/5+}$ nanotubes at pH of 2, and the spectra of the monomeric porphyrins at the same pH: suspension of SnTPyP^{2+} monomer (black), $H_4TPPS_4^{2-}$ monomer (red), and nanotubes (green). (Inset) Transmission electron microscope image of the porphyrin nanotubes. Reprinted with permission from Reference 17. © 2004 American Chemical Society. (b) UV–visible absorption spectra of a suspension of the Zn/Sn nanosheets (red) that is deposited on a glass slide (dark) for comparison with the spectra of the constituent porphyrins in solution (dashed gray) and a spectrum of the analogous Zn/Sn clover-like structures (green).[20] From (a) and (b), a red shift in the absorption bands is observed for the J-aggregate band of the ionic self-assembly porphyrin nanostructures, suggesting the coherent coupling of the transition dipoles that results in intense resonant light scattering at these wavelengths. (c) Atomic force microscope (AFM) image of a ZnTPPS^{4-}/SnT(*N*-EtOH-4-Py)P^{4+}clover (image is 5 μm × 5 μm). Inset: Tunneling AFM (TUNA) current–voltage curve for conduction through the clover from the *p*-doped conductive Si substrate when illuminated with cool white light. The voltage was swept from –12 V to +12 V (red line) and from +12 V to –12 V (blue line) with a voltage step of 0.25 V. Reprinted with permission from Reference 18. © 2010 American Chemical Society. (d) AFM images of ZnTPPS^{4-} and SnT(*N*-EtOH-4-Py)P^{4+} nanosheets. Inset: (i) Current versus voltage curves under visible light illumination and (ii) the numbered points indicate AFM positions at which the current curves were measured (not all shown). The voltage was swept from –12 V to +12 V (red line) and from +12 to –12 V (black line) with a voltage step of 0.25 V. Data were obtained in contact mode under visible light illumination and in the dark (data not shown). The inset plots in (c) and (d) show that photoconductivity of the binary ionic nanomaterials reveals the electron-transfer processes. The excited state of the Zn porphyrin can reduce the SnP to the radical anion, leaving a hole on the Zn porphyrin and leading to free charge carriers and a photocurrent.[20] Note: UV, ultraviolet; H_4TPPS^{2-}, meso-tetrakis(4-sulfonatophenyl) porphyrin; SnT(*N*-EtOH-4-Py)P^{4+}, Sn(IV) tetrakis(*N*-ethanol-4-pyridyl) porphyrin; $(MTPPS_4)^{4-}$, water-soluble porphyrins (M = 2H, Sn, Cu, Ni, Ag, and Zn); SnTHPyP$^{4+/5+}$, Sn (IV) tetrakis(4-pyridyl) porphyrin; Et, ethyl; Py, pyridyl; Me, methyl; P, porphyrin.

Two intense bands at 496 nm and 714 nm appeared, suggesting the J-aggregate bands were redshifted relative to the bands of monomeric porphyrins.[17] The UV-visible absorption spectra of Zn/Sn nanosheets and clovers showed redshifted J-aggregate bands of the clovers at 459 nm. Part of the intensity is because of resonance light scattering rather than light absorption.[20] The nanosheets show no α and β bands, which result when the intense Soret band splits into two at 420–490 nm, suggesting there are no extended slipped π–π stacks, which are intermolecular delocalization coupling electrons. The monomeric solution contribution is significant for the nanosheets, so nanosheets deposited onto a glass slide also showed a redshift in the absorption bands, but the shift was smaller than for the J-aggregate band of the clovers, suggesting weaker coupling of the transition dipoles (Figure 3b).

ISA porphyrin nanostructures of oppositely charged porphyrin molecules are of interest for carrying out the light-harvesting and electron-transfer processes for applications in electronic devices. The electrostatic stabilization of charge-separated holes and electrons may be conducive to electron transfer and formation of free charge carriers, and the spatial organization in the solid plays a major role in determining the electronic properties. For example, atomic force microscopy (AFM) studies of individual Zn/Sn clovers (Figure 3c) revealed significant photoconductivity between the conducting doped Si substrate and the conducting tip at a point on the top surface of the clover (i.e., through the clover).[18,21,22] This can be seen from the current–voltage curve (inset in Figure 3c). When the bias of the applied potential was switched, no photocurrent was observed up to 12 V, and there was only a low constant residual current in the dark for either bias condition.

Conductivity measurements and AFM images of 65-nm-thick Zn/Sn nanosheets were also obtained, as shown in Figure 3d. A much smaller current was detected for either bias, and the current was unaltered when the nanosheet was irradiated with visible light, thus the current path normal to the surface is insulating. The nanosheets and clovers are thus insulators and photoconductors, respectively.[21] Altering the metals in the porphyrins could vary cooperative interactions between the porphyrin subunits and could then alter the electronic and photophysical properties of these solids, which leads to tunable functionality. Photoconductivity studies of the porphyrin nanostructures are important for potential applications in optoelectronic devices. Along with these experiments, their photoconductive behavior makes them excellent candidates for chemical-sensing applications.

Photocatalytic properties and applications of ISA porphyrin nanostructures

Self-assembled porphyrin nanostructures provide a new type of material for optoelectronic and photochemical applications.

https://doi.org/10.1557/mrs.2019.40 Published online by Cambridge University Press

In particular, these materials are of interest for carrying out light-harvesting and charge-separation and transport processes in artificial photosynthesis systems, as shown in **Figure 4**a. For example, after absorption of visible or UV light, the Sn porphyrin forms a long-lived excited triplet state, SnP*, and then it is rapidly reduced by an ED, such as ascorbic acid, and forms a long-lived radical anion SnP^{-}. The SnP^{-} anion is a strong reductant (SnP/SnP^{-}, –0.66 V) that is capable of efficiently reducing a variety of metal ions, including Ag, Au, Hg, Pb, Cu, and Pt to zero valent metals.[23,24] For example, Sn porphyrin nanotubes were used to photoreduce the negatively charged Au (I)-thiosulfate complex, which formed gold particles mainly on the outer surfaces of the tubes (Figure 4b[i]). On the other hand, upon photoreducing the positively charged Au(I)-thiourea complex, the metal grew exclusively within the hollow interior of the nanotubes to form a continuous polycrystalline gold nanowire with an external ball (Figure 4b[ii]).[24] These results suggest that directional electron/energy transport within the tube walls and the electrostatic interactions between the metal complex and ISA nanostructure surfaces may determine the marked regiospecificity of metal growth.

After Pt self-metallization of these nanostructures, electrons from the photogenerated π-anion radicals can reduce protons to hydrogen at catalytic Pt metal nanoparticles in the presence of an ED using sunlight. As shown by the expanded curves (yellow squares and circles) for the Zn/Sn clovers in Figure 4c, the platinized clovers from the suspensions used in the H_2 generation experiments were nearly unchanged by the reaction, even after 14 days of continuous illumination. Some H_2 was generated even without the use of the electron relay, implying that reducing equivalents may reach the platinum nanoparticles directly through the clovers instead of via reduced methyl viologen in solution.[25] Pt nanoparticles residing on the surface of the ISA solid could enhance water reduction efficiency and stability by direct transfer of electrons in the presence of a sacrificial ED.

Self-assembled porphyrin nanostructures offer new opportunities for the reduction of carbon dioxide to precursors for carbon-based liquid fuels. ISA nanostructures containing cobalt and zinc porphyrins might use the photoexcited zinc porphyrin to reduce the cobalt porphyrin to the active Co (I) species directly, and the Zn porphyrin cation might be chemically reduced back to the resting neutral state by a redox couple that also drives O_2 evolution, as shown in Figure 4d.[22] The potential for CO_2 reduction using an aqueous electrolyte is considerably lower than for nonaqueous systems (~ –1 V versus –2 V, respectively), and negligible amounts of side products (e.g., formate) are produced. With the advent of ISA nanocomposites, it may be possible to grow CO_2-reduced ISA nanocatalysts on a light-active cooperative binary ionic structure that provides the required reducing equivalents. The carbon monoxide produced provides a convenient feedstock for the production of carbon-based fuels through syngas reactions.

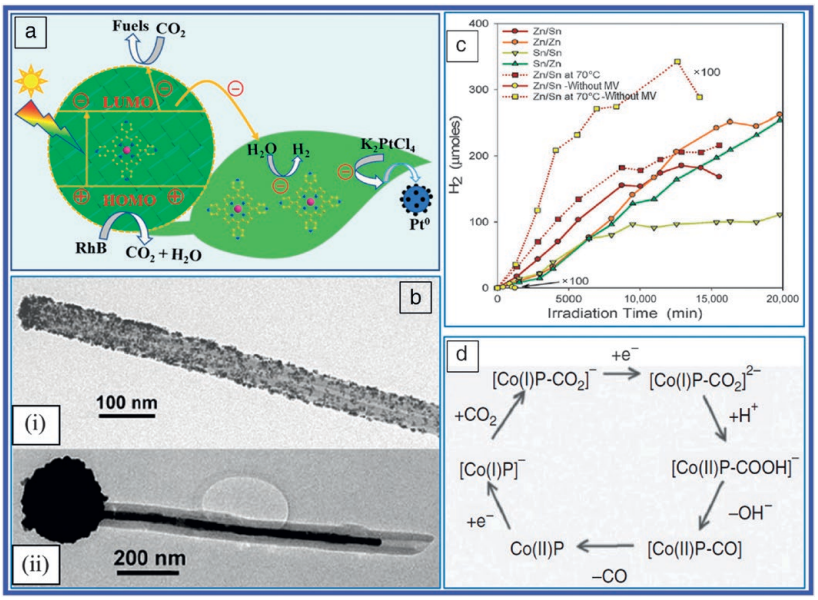


Figure 4. (a) The schematic of photocatalytic applications of ionic self-assembly porphyrin nanostructures. (b) Transmission electron microscope images of (i) a platinized porphyrin nanotube with Pt nanoparticles distributed mainly on the outside surface and (ii) a gilded nanotube obtained using the Au(I)-thiourea complex. Reprinted with permission from Reference 23. © 2004 American Chemical Society. (c) Total H_2 generated by the platinized porphyrin clovers (Zn/Sn, Zn/Zn, Sn/Sn, Sn/Zn) grown at room temperature (solid lines) and at 70°C for the Zn/Sn clovers (dotted lines) versus irradiation time with visible light from a tungsten lamp. Zn/Sn clovers with (dark red symbols) and without (yellow) methyl viologen (MV). The latter are expanded by a factor of 100. Despite the differences in morphology and composition for the clovers, all of the structures produce H_2 at similar initial rates. It is possible that better crystallinity of the 70°C Zn/Sn clovers further enhanced exciton or charge migration, resulting in greater H_2 production than that for room-temperature clovers. The cooperative behavior of the binary solids may play an important role in the relative activities and durabilities of the clovers. Reprinted with permission from Reference 25. © 2011 Royal Society of Chemistry. (d) Reaction mechanism for CO_2 reduction by cobalt porphyrin-modified electrodes determined from quantum chemical calculations. Reprinted with permission from Reference 22. © 2013 Wiley. Note: UV, ultraviolet, P, porphyrin; LUMO, lowest unoccupied molecular orbit; HOMO, highest occupied molecular orbit.

Conclusions

Binary porphyrin systems that are ionically self-assembled are promising candidates for the fabrication of high-performance electronic and optical devices, by integrating microscopic, spectroscopic, and light-harvesting properties of different porphyrin assemblies of alternating ionic tectons (the macrocycles and their ring substituents), held together by electrostatic interactions, hydrogen bonding, and π–π interaction. This combination of chemical and structural factors potentially allows a high degree of control over the cooperative interactions between the porphyrin cores (e.g., charge transfer) and, consequently, the functionality

https://doi.org/10.1557/mrs.2019.40 Published online by Cambridge University Press

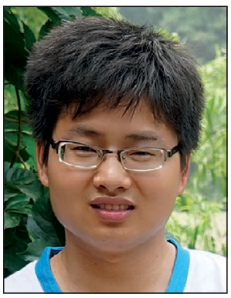
(e.g., charge separation and migration) of the organic solid and provides further understanding of the chemical and biochemical reaction procedures. These new materials are anticipated to have applications in solar-energy technologies and organic electronics and optoelectronics. More work is necessary to advance the understanding of the structure–function relationship of porphyrin nanostructures, which will enable tailoring of their properties for a particular application.[26] Such studies will also help in gaining better control over the synthetic architecture of these materials and building high-performance, stable, and durable molecular devices. Developing these relationships remains one of the foremost scientific challenges for advancing porphyrin optoelectronic technology.

Acknowledgments

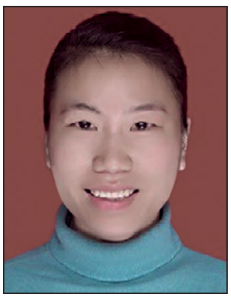
Y.Z. acknowledges support from the National Natural Science Foundation of China (21802032), the Program for Changjiang Scholars, and the Innovative Research Team in University, Henan Province (No. PCS IRT_15R18).

References

1. C.M. Drain, A. Varotto, I. Radivojevic, *Chem. Rev.* **109**, 1630 (2009).
2. Y. Chen, A. Li, Z. Huang, L. Wang, F. Kang, *Nanomaterials* **6**, 51 (2016).
3. E. Shevchenko, D. Talapin, N. Kotov, S. O'Brien, C. Murray, *Nature* **439**, 55 (2006).
4. C. Zhang, P. Chen, H. Dong, Y. Zhen, M. Liu, W. Hu, *Adv. Mater.* **27**, 5379 (2015).
5. H. Ju, X. Zhang, J. Wang, in *NanoBiosensing Principles, Development and Application*, H. Ju, X. Zhang, J. Wang, Eds. (Springer, New York, 2011), pp. 111–146.
6. T. Hasobe, H. Sakai, in *Chemical Science of π-Electron Systems*, T. Akasaka, A. Osuka, S. Fukuzumi, H. Kandori, Y. Aso, Eds. (Springer, Tokyo, 2015), pp. 475–491.
7. Z. Wang, Z. Li, C.J. Medforth, J.A. Shelnutt. *J. Am. Chem. Soc.* **129**, 2440 (2007).
8. S. Hiroto, Y. Miyake, H. Shinokubo, *Chem. Rev.* **117**, 2910 (2017).
9. J. Wang, Y. Zhong, X. Wang, W. Yang, F. Bai, B. Zhang, L. Alarid, K. Bian, H. Fan, *Nano Lett.* **17**, 6916 (2017).
10. J. Wang, Y. Zhong, L. Wang, N. Zhang, R. Cao, K. Bian, L. Alarid, R.E. Haddad, F. Bai, H. Fan, *Nano Lett.* **16**, 6523 (2016).
11. Y. Zhong, J. Wang, R. Zhang, W. Wei, H. Wang, X. Lü, F. Bai, H. Wu, R. Haddad, H. Fan, *Nano Lett.* **14**, 7175 (2014).
12. P.L. Marek, in *Biomimetic Dye Aggregate Solar Cells*, P.L. Marek, Ed. (Springer International, New York, 2013), pp. 27–90.
13. A. Pichon, *Nat. Chem.* **2**, 611 (2010).
14. L.G. De, A. Romeo, V. Villari, N. Micali, I. Foltran, E. Foresti, I.G. Lesci, N. Roveri, T. Zuccheri, L.M. Scolaro, *J. Am. Chem. Soc.* **131**, 6920 (2009).
15. K.W. Hipps, U. Mazur, J.R. Eskelsen, M. Adinehnia, in *Handbook of Porphyrin Science*, K.W. Hipps, U. Mazur, J.R. Eskelsen, M. Adinehnia, Eds. (World Scientific, Singapore, 2016), pp. 69–103.
16. Z. Wang, K. Ho, C. Medforth, J. Shelnutt, *Adv. Mater.* **18**, 2557 (2006).
17. Z. Wang, C. Medforth, J. Shelnutt, *J. Am. Chem. Soc.* **126**, 15954 (2004).
18. K. Martin, Z. Wang, T. Busani, R. Garcia, Z. Chen, Y. Jiang, Y. Song, J. Jacobsen, T. Vu, N. Schore, B. Swartzentruber, C. Medforth, J. Shelnutt, *J. Am. Chem. Soc.* **132**, 8194 (2010).
19. Z. Wang, L. Lybarger, W. Wang, C. Medforth, J. Miller, J. Shelnutt, *Nanotechnology* **19**, 395604 (2008).
20. Y. Tian, C. Beavers, T. Busani, K. Martin, J. Jacobsen, B. Mercado, B. Swartzentruber, F. van Swol, C. Medforth, J. Shelnutt, *Nanoscale* **4**, 1695 (2012).
21. J. Shelnutt, Y. Tian, K. Martin, C. Medforth, in *Handbook of Porphyrin Science*, J. Shelnutt, Y. Tian, K. Martin, C. Medforth, Eds. (World Scientific, Singapore, 2013), pp. 227–277.
22. J. Shelnutt, C. Medforth, in *Organic Nanomaterials: Synthesis, Characterization, and Device Applications*, T. Torres, G. Bottari, Eds. (Wiley, Hoboken, NJ, 2013), pp. 103–130.
23. Z. Wang, C. Medforth, J. Shelnutt, *J. Am. Chem. Soc.* **126**, 16720 (2004).
24. C. Medforth, Z. Wang, K. Martin, Y. Song, J. Jacobsen, J. Shelnutt, *Chem. Commun.* **47**, 7261 (2009).
25. Y. Tian, K. Martin, J. Shelnutt, L. Evans, T. Busani, J. Miller, C. Medforth, J. Shelnutt, *Chem. Commun.* **47**, 6069 (2011).
26. C.J. Medforth, F.B. van Swol, in *Office of Scientific & Technical Information Technical Reports* (Sandia National Laboratories, Albuquerque, NM, 2010), pp. 4–10. □



Yong Zhong is currently an associate professor at the Key Laboratory for Special Functional Materials of the Ministry of Education at Henan University, China. He received his PhD degree in organic chemistry from Henan University in 2017. His research focuses on the nanostructure-based self-assembly of porphyrin and Z-scheme photocatalytic systems. Zhong can be reached by email at zhywy8521115@163.com.



Jiefei Wang is currently an associate professor at the International Joint Center for Biomedical Innovation at Henan University, China. She received her PhD degree in inorganic chemistry from Henan University in 2017. Her research focuses on the applications of biofunctional materials in tumor imaging, therapy, and drug delivery, and includes the design of photosensitizer materials, rare-earth nanomaterials, gadolinium contrast nanomaterials, and detecting tumors through diagnostics. Wang can be reached by email at jfwang@henu.edu.com.



Yongming Tian is a senior scientist at Angstrom Thin Film Technologies LLC. He received his PhD degree in materials engineering in 2013 from the New Mexico Institute of Mining and Technology. His research focuses on nanostructures and ultrathin membranes for applications in emerging energy technologies. Tian can be reached by email at yongming.tian@gmail.com.

JOIN OR RENEW TODAY!
mrs.org/membership
Your MRS Membership includes online access to ALL MRS journals.



https://doi.org/10.1557/mrs.2019.40 Published online by Cambridge University Press